"People" meet "Markovians"—Individual-based modelling with hybrid stochastic systems

MOLLY HAWKER

School of Computer Science and Mathematics (CSM)
Liverpool John Moores University (LJMU)
Byrom Way, Liverpool L3 3AF, United Kingdom
M.A.Hawker@2021.ljmu.ac.uk

IVO SIEKMANN

School of Computer Science and Mathematics (CSM)
Liverpool John Moores University (LJMU)
Byrom Way, Liverpool L3 3AF, United Kingdom
i.siekmann@ljmu.ac.uk

Liverpool Centre for Cardiovascular Science
Liverpool
United Kingdom

Data Science Research Centre
Liverpool John Moores University (LJMU)
United Kingdom

PROTECT-eHealth
Liverpool John Moores University (LJMU)
Liverpool
United Kingdom

Received (13^{th} April 2023)
Accepted (16^{th} November 2023)

Individual-based models (IBM) enable modellers to avoid far-reaching abstractions and strong simplifications by allowing for a state-based representation of individuals. The fact that IBMs are not represented using a standardised mathematical framework such as differential equations makes it harder to reproduce IBMs and introduces difficulties in the analysis of IBMs. We propose a model architecture based on representing individuals via Markov models. Individuals are coupled to populations—for which individuals are not explicitly represented—that are modelled by differential equations. The resulting models consisting of continuous-time finite-state Markov models coupled to systems of differential equations are examples of piecewise-deterministic Markov processes (PDMP). We will demonstrate that PDMPs, also known as hybrid stochastic systems, allow us to design detailed state-based representations of individuals which at the same time can be systematically analysed by taking advantage of the theory of PDMPs. We will illustrate design and analysis of IBMs using PDMPs via the example of a predator that intermittently feeds on a logistically-growing prey by stochastically switching between a

resting and a feeding state. This simple model shows a surprisingly rich dynamics which, nevertheless, can be comprehensively analysed using the theory of PDMPs.

Keywords: individual-based model; agent-based model; Markov model; piece-wise deterministic Markov process (PDMP); hybrid stochastic system.

1. Introduction

Individual- or agent-based models have become increasingly popular and are successfully applied in a variety of disciplines—for the field of ecology as well as for a general introduction, see the monographs by Grimm and Railsback.[1,2] To illustrate the vast scope of individual-based models (IBM) we refer to applications in disciplines such as epidemiology[3,4] where IBMs have been used for modelling explicitly how infections spread along a contact network, most recently including detailed representations of the behaviour of individuals.[5] Moreover, in cell biology, Osborne et al.[6] provide an overview how various cellular processes within multicellular tissues can be represented with different modelling approaches. Land-use modelling combines environmental aspects with economic implications and individual decision-making.[7] IBMs have also been applied in social psychology to investigate the formation of sexual partnerships.[8] A special issue, recently edited by Siekmann and Osborne,[9] contains applications in modelling of chemical reactions,[10] developmental biology[11] and ecology.[12,13]

Explicit representations of individuals in a population of humans, organisms or cells help the modeller to avoid making far-reaching abstractions and strong simplifications which would be necessary when applying traditional mathematical modelling approaches such as differential equations. This led Musters et al.[12] to propose that IBMs will play a central role in developing more predictive models in ecology by emphasising an organism-based in contrast to a species-based approach. Describing an individual via a set of states enables the modeller to track the current situation of each individual at a high level of detail. In contrast, population-based models based on differential equations describe the amount of members of a population which are, implicitly, assumed to all be in the same state or that this state doesn't matter. By defining transitions between states using approaches such as a system of highly complex interdependent rules, IBMs can describe individuals who respond adaptively to their environment by making "intelligent" decisions based on the current state of the environment. This is much harder, if not impossible, using differential equations.

In principle, there are hardly any restrictions how the transitions between the states of an IBM can be formulated. This is, on the one hand, one of the main benefits of IBMs—rather than having to design a model according to the requirements of a more restrictive underlying modelling framework, it is possible to fine-tune the transition rules so that they reflect as well as possible the behaviour of the "real" individual to be modelled.

On the other hand, this flexibility is the reason for some of the main challenges

of the IBM approach, such as the reproducibility of the results and the difficulty of systematical analysis of IBMs. Unlike for models that are based on differential equations IBMs are not based on a common mathematical framework so that there is, inevitably, more room for ambiguity as well as an increased risk of omitting essential details in the model description of an IBM. Similarly, because IBMs are not built according to a fixed mathematical template, a powerful theory such as dynamical systems theory for differential equations does not exist. This lack of a general theory of IBMs makes the analysis of IBMs time-consuming—the modeller might have no choice but run a lot of simulations in order to gain sufficient insight into the model behaviour. Also, it is harder to determine how robust an IBM is to changes of the modelling assumptions.

These issues have long been recognised in the field as evidenced by strong efforts to standardise IBMs as well as developing methods for facilitating their analysis which are summarised in a recent review.[14] In order to address the problem of reproducibility, the Overview, Design concepts and Details (ODD) protocol has been developed. The goal of the ODD protocol is to improve reproducibility of IBMs by standardising the description of IBMs.[15–17] The same authors developed TRACE (TRAnsparent and Comprehensive model Evaluation), a framework for describing the model development cycle itself.[18] Using TRACE, modellers make explicit why they made which specific design choices during the development of the IBM. This provides some indication how robust the model would be to variations in the modelling assumptions. This helps to clarify which considerations were behind various changes to the model structure.

Although protocols are available that enable modellers to appropriately describe IBMs, another consequence of each IBM being, ultimately, one of a kind, is that, unlike for more structured modelling approaches, no general theoretical framework for the analysis of IBMs exists. For systematically investigating how an IBM responds to parameter variations there seems to be no alternative to exhaustive simulations, which is computationally prohibitive for more complex IBMs. In contrast, for analysing models based on differential equations, dynamical systems and bifurcation theory[19,20] provide a highly successful general framework. Although for many practical examples of models it might not be possible to carry out the calculations required for an analytical bifurcation analysis, continuation techniques can be applied for carrying out a numerical bifurcation analysis, using software such as AUTO[21] or MATCONT.[22,23]

One might wonder if there is a way to adapt dynamical systems analysis to IBMs by defining appropriate aggregate or "macroscopic" quantities, for example, by calculating the total number of predator or prey or summarising all individuals that are susceptibles, infected or resistant. At first glance, it does not seem to be possible to apply bifurcation analysis to "macroscopic" quantities derived from an IBM because these techniques seem to rely on calculations that are directly applied to the differential equations defining a model. However, numerical continuation does, in fact, only evaluate how the values of the quantities described by a system of differ-

ential equations respond to parameter variations. This observation led Kevrekidis and co-workers to develop "equation-free modelling", a highly original approach that allows us to apply bifurcation analysis to IBMs using numerical continuation. Although "equation-free modelling" is very promising it is not easy to implement in practice and there are still relatively few applications to IBMs.[24–29]

Given that the analysis of IBMs is a considerable challenge, one might wonder if constraining the flexibility of a rule-based approach for updating the states of individuals might enable us to take advantage of explicit modelling while at the same time providing an underlying mathematical structure that is essential for developing approaches for systematically investigating these models. Examples for modelling frameworks that have a constrained architecture which facilitates their analysis include branching processes[30] and active Brownian particles.[31] Branching processes enable us to track the "family tree" i.e. the descendance structure of individuals within a population, and active Brownian particles enable us to investigate simple agents moving in a spatial domain which can show surprisingly complex behaviour such as the formation of swarms. However, both approaches provide very limited representations of individuals unless they are augmented by additional states for describing the individuals.

The purpose of the study presented here is to develop a detailed state-based representation of individuals that is, at the same time, amenable to systematic mathematical analysis. Because we will describe individuals using Markov models we will, in the following, refer to this species as "the Markovian", in contrast to "the people" which we call populations for which an individual-based description is not required. A modelling framework that aims to combine the strengths of IBMs and population-based model is very much in line with Siekmann & Osborne[9] where we argue that a synthesis of population-based models and IBMs is the most promising approach for investigating the role of individuals in various scientific disciplines.

Markov models allow us to describe an individual by a set of states $\mathcal{S} = \{S_1, \ldots, S_n\}$. The model structure can be represented as a graph—the nodes of the graphs are the various possible states of the individual and the edges define which transitions between states S_i and S_j are possible. Until this point, the model structure of a Markov model is completely analogous to a general IBM. However, whereas in a Markov model the stochastic transitions between states can only be represented by transition rates, a general IBM allows for a rule-based description. Before we introduce our approach for designing IBMs using Markov models we would like to discuss some previous studies that have related Markov chain theory to IBMs. Izquierdo et al.[32] propose a computational approach that attempts to describe the stochastic dynamics of a given IBM by fitting a Markov model to the observed distributions over the states of the model obtained from simulations. In an appendix, they also investigate the qualitative dynamics of several IBMs using Markov chain theory without explicitly fitting to simulations of the model. Laubenbacher et al.[33] suggest to take stochastic finite dynamical systems as the theoretical foundation of IBMs which they present as Markov chains with additional structure.

However, this idea does not seem to have been pursued further since it has been proposed—Laubenbacher et al.[33] restrict their presentation to deterministic finite dynamical systems. The main motivation of Banisch et al.[34] and Banisch[35] is to take advantage of Markov chain theory to derive the behaviour of a population—their chosen application is the formation of opinions—whose individuals are described using Markov models.

These previous studies primarily aim to take advantage of Markov chain theory as a tool for analysing IBMs more rigorously—an exception is Mooij et al.[36] who developed an IBM based on a Markov model that was, however, ultimately only used as a deterministic matrix model that described deterministic transitions of fractions of a population rather than explicitly modelling individuals. In contrast, we propose to design IBMs using Markov models. Also, in addition to describing individuals using a Markov model, our approach enables us to consider additional populations represented using a system of ordinary differential equations (ODE). Whilst representing state transitions via transition rates is less flexible than a rule-based approach, imposing these constraints has clear benefits when it comes to analysing the model behaviour. There is a well-developed theory for Markov models that enables us, based on a rigorous mathematical theory, to characterise many features of the stochastic dynamics such as the average time that a model spends in a particular state (sojourn time), the time it takes, on average, to reach a particular state S_j from an initial state $S^0 = S_i$ (first passage time) as well as the probability distribution $\boldsymbol{\pi}$ over the state set $\mathcal{S}$ for $t \to \infty$ (limiting distribution). In contrast, for a general IBM, due to the fact that each model has its own idiosyncratic structure, the approach to analysing the model can, at least initially, only be based on heuristic ad-hoc approaches and a framework for carrying out a systematic analysis needs to be developed, at least to some extent, from scratch whenever a new model is investigated.

In order to demonstrate our approach, we will, throughout this article, consider the very simple example of a fish that feeds on zooplankton. Initially, the fish will switch between only two behavioural states, a resting state R and a feeding state F. We assume that for the plankton population, an individual-based description is not required, so that we will only account for the size of the population x which will be described by an ordinary differential equation (ODE). Thus, in this example, we observe a "showdown" of "Markovian" fish and the "people", a plankton population.

Models that consist of a continuous-time finite-state Markov model coupled to a system of ODEs have been introduced by Davis[37] who named them piecewise-deterministic Markov processes (PDMP). They are a special case of a general class of processes referred to as hybrid stochastic systems, see Maclaurin and Bressloff[38] for a recent review. Moreover, the two volumes of the book by Bressloff[39,40] contain a lot of applications of stochastic hybrid systems in the context of cell biology. A related class of deterministic models are the models developed by Krivan in a series of articles[41–43] where a predator switches between different prey populations based on optimising the energy intake that can be obtained from each of the prey species.

Based on the theory of PDMPs/hybrid stochastic systems we can calculate the probability densities for each state of the Markov model over time and dependent on the prey population x. We have deliberately chosen a model that is simple enough so that the stationary distributions of the resting and the feeding state, $\rho^{\infty}_{\mathrm{R}}(x)$ and $\rho^{\infty}_{\mathrm{F}}(x)$ ca be calculated analytically. In practice, for most models the probability densities cannot be calculate analytically. In that case, the partial differential equations (PDE) for the probability densities can be solved numerically.[44]

In section 3.1 and 3.2 we will study our simple model for a predator that switches between resting R and feeding F for various choice of the switching rates k_{RF} and k_{FR} ranging over several orders of magnitude. We will then investigate several extensions of our model. In section 3.3.1 we will make the switching rates k_{RF} and k_{FR} dependent on the prey population x. The states $S \in \mathcal{S}$ of the finite state Markov model representing the predator only account for ordinal states that account, for example, for different behavioural states of the predator. In section 3.3.2 we will consider an example for a continuous state of the predator which can be described by a ODE. We introduce an energy level E that depends on the amount of prey that is consumed by the predator over time. Finally, whereas for most of the article we only consider one predator, adding more predators can be easily achieved by combining multiple copies of the infinitesimal generator that has previously been developed for representing one predator. Finally, we discuss our results in section 4.

2. Methods

We illustrate our approach using a very simple example. Consider a population x for which we assume that modelling each individual explicitly would not be warranted so that it can be represented by a differential equation. Let us assume that this population grows logistically and interacts with one (or more) individual(s) which are represented by a continuous-time Markov model that describes the transitions between two states, a resting state R and a feeding state F. Then the continuous-time Markov model representing the stochastic transitions between the resting and the feeding state is

$$\frac{d\mathbb{P}(t; S = \mathrm{R}, \mathrm{F})}{dt} = \mathbb{P}(t; S = \mathrm{R}, \mathrm{F}) \cdot \underbrace{\begin{pmatrix} -k_{\mathrm{RF}} & k_{\mathrm{RF}} \\ k_{\mathrm{FR}} & -k_{\mathrm{FR}} \end{pmatrix}}_{\mathbf{Q}_{\mathrm{RF}}}. \tag{2.1}$$

where $\mathbf{Q}_{\mathrm{RF}}$ is the so-called infinitesimal generator of the Markov model. Suppose now that the individual feeds on the population x with rate d but only when in the feeding state F. Then the population dynamics of x is described by the differential equation

$$\frac{dx}{dt} = \begin{cases} x(1-x) =: f_{\mathrm{R}}(x), & S = \mathrm{R} \\ x(1-x) - dx =: f_{\mathrm{F}}(x), & S = \mathrm{F} \end{cases} \tag{2.2}$$

After coupling the Markov model (2.1) to the differential equation (2.2), the resulting system can again be considered as a Markov process where the state

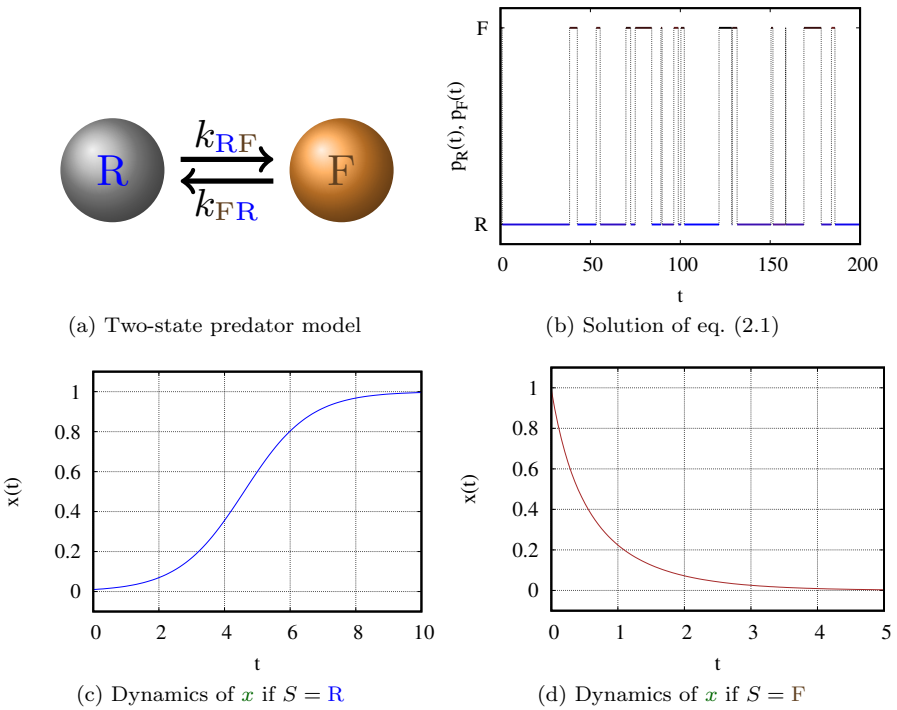

(a) Two-state predator model

(b) Solution of eq. (2.1)

(c) Dynamics of x if $S = \mathrm{R}$

(d) Dynamics of x if $S = \mathrm{F}$

Fig. 1: Dynamics of the model shown in (a) which represents a predator that stochastically switches between a resting state R and a feeding state F with the transition rates k_{RF} and k_{FR}. A realisation of the dynamics of this model is shown in (b). Interactions of the predator with a prey population x are represented by the equation (2.2) which describes the dynamics of x depending on the state of the predator. When the predator is in the resting state R the prey grows logistically as shown in (c). In contrast, when the predator is in the feeding state F it is assumed that it feeds with a linear catch rate d that exceeds the growth rate of the prey so that the prey population decreases as in (d). As the predator stochastically switches between R and F the solution of (2.2) is pieced together from deterministic segments as in (c) and in (d). That is why models such as (2.2) are called piece-wise deterministic Markov processes (PDMP).

space of the original Markov process $\mathcal{S} = \{\mathrm{R}, \mathrm{F}\}$ has been augmented by the prey population x. Because for each t the probability of a state $(S \in \mathcal{S}, x \in [0, 1])$ of (2.2) depends on the continuous variable x, it is described in terms of probability densities $\boldsymbol{\rho}_{\mathrm{RF}}(t) = (\rho_{\mathrm{R}}(t), \rho_{\mathrm{F}}(t))$. The derivation of an advection equation that can be used for calculating $\boldsymbol{\rho}_{\mathrm{RF}}(t)$ is very clearly explained by Tveito and Lines[45] albeit in the context of a completely different application. This equation is the differential form of the *Chapman-Kolmogorov* (CK) equation for PDMPs[37] which is derived by

van Kampen[46] from the CK equation.

$$\frac{\partial}{\partial t}\boldsymbol{\rho}_{\mathrm{RF}}(t,x) + \underbrace{\frac{\partial}{\partial x}\begin{pmatrix} f_{\mathrm{R}}(x)\cdot\rho_{\mathrm{R}}(t,x), \\ f_{\mathrm{F}}(x)\cdot\rho_{\mathrm{F}}(t,x). \end{pmatrix}}_{\text{dynamics of } x} = \underbrace{\boldsymbol{\rho}_{\mathrm{RF}}(t,x)\cdot\mathbf{Q}_{\mathrm{RF}}}_{\text{transitions R, F}}. \tag{2.3}$$

Rather than reproducing Tveito's and Lines'[45] derivation of the differential CK equation (2.3) from a conversation law for the probability density $\boldsymbol{\rho}_{\mathrm{RF}}$, we illustrate the equation using a few remarks:

(1) If there is no change in the population x, i.e. if $f_{\mathrm{R}}(x) = f_{\mathrm{F}}(x) = 0$, (2.3) reduces to equation (2.1).

(2) Let us consider the distribution of the state F. The density $\rho_{\mathrm{F}}(t,x)$ decreases by the rate $-k_{\mathrm{FR}}\rho_{\mathrm{F}}(t,x)$ which accounts for transitions from F to R. At the same time, $\rho_{\mathrm{F}}(t,x)$ increases due to transitions from R to F by $k_{\mathrm{RF}}\rho_{\mathrm{R}}(t,x)$. Altogether, we find that the rate of change for $\rho_{\mathrm{F}}(t,x)$ is

$$\frac{\partial\rho_{\mathrm{F}}(t,x)}{\partial t} = -k_{\mathrm{FR}}\rho_{\mathrm{F}}(t,x) + k_{\mathrm{RF}}\rho_{\mathrm{R}}(t,x). \tag{2.4}$$

This equation describes the balance of the probability densities for the two states F and R. It can, of course, be generalised to more than two states in a straightforward way.

(3) For the dependency of ρ_{F} on the prey population x, we consider how $\rho_{\mathrm{F}}(t,x)$ changes at the value $x = x_0$. According to (2.2), the first derivative of the population x_0 is $f(x_0)$. Thus—because x_0 increases or decreases with the rate $f(x_0)$ and analogous to our analysis of the state F above—the density of $\rho_{\mathrm{F}}(t,x_0)$ decreases with the rate $-f(x_0)\cdot\rho_{\mathrm{F}}(t,x_0)$. Apart from this negative contribution, the density $\rho_{\mathrm{F}}(t,x_0)$ increases due to transitions to $x = x_0$ from population levels x' close to x_0—in contrast to the situation in (2.4) where we only had to consider a discrete set of states, the prey population x defines a continuous state set and the transitions from prey levels close to x_0 can be quantified by the derivative of the function $-f(x)\cdot\rho_{\mathrm{F}}(t,x)$. Thus, we obtain for the rate of change for $\rho_{\mathrm{F}}(t,x)$ due to changes in the variable x:

$$\frac{\partial\rho_{\mathrm{F}}(t,x)}{\partial t} = \frac{\partial}{\partial x}[-f(t,x)\cdot\rho_{\mathrm{F}}(t,x)]. \tag{2.5}$$

Our considerations show that (2.5) simply is a continuous version of (2.4).

(4) Combining (2.4) and (2.5) we obtain the differential Chapman-Kolmogorov equation (2.3).

Because we are primarily interested in the long-term behaviour i.e. $t \to \infty$ we will focus, in particular, on the asymptotic densities $\rho_{\mathrm{R}}^{\infty}(x)$ and $\rho_{\mathrm{F}}^{\infty}(x)$. These densities are obtained by setting $\frac{\partial}{\partial t}\boldsymbol{\rho}_{\mathrm{RF}}(t,x) = \mathbf{0}$ and solving the resulting system of ordinary differential equations. For the simple example investigated in this study these differential equations can be solved analytically. For the analysis it is important to consider if $f_{\mathrm{F}}(x)$ changes sign for $x \in [0,1]$ ($f_{\mathrm{R}}(x)$ is always positive on the interval

$[0,1]$). This depends on the catch rate d, where three cases for the catch rate d need to be distinguished, $d > 1$, $d = 1$ and $d < 1$. Let us first look at $d > 1$ and $d < 1$. As shown in Appendix A we obtain, for $x \in [0,1]$ for $d > 1$ and $x \in [1-d, 1]$ for $d < 1$:

$$\rho_{\mathrm{R}}^{\infty}(x) \propto x^{\frac{k_{\mathrm{FR}}}{d-1}-k_{\mathrm{RF}}-1}(1-x)^{k_{\mathrm{RF}}-1}(x+d-1)^{-\frac{k_{\mathrm{FR}}}{d-1}}, \tag{2.6}$$

$$\rho_{\mathrm{F}}^{\infty}(x) \propto x^{\frac{k_{\mathrm{FR}}}{d-1}-k_{\mathrm{RF}}-1}(1-x)^{k_{\mathrm{RF}}}(x+d-1)^{-\frac{k_{\mathrm{FR}}}{d-1}-1}. \tag{2.7}$$

Outside these intervals we have $\rho_{\mathrm{R}}^{\infty}(x) = \rho_{\mathrm{F}}^{\infty}(x) = 0$. This can be explained as follows: For $d > 1$, $f_{\mathrm{F}}(x)$ is negative on $[0,1]$; therefore we obtain a solution for the complete interval $[0,1]$. For $d < 1$, $f_{\mathrm{F}}(x)$ is positive for $x < 1-d$ and negative for $x > d-1$. But this means that if we initially start with $x < 1-d$ the prey population x will grow until it eventually exceeds $x = 1-d$ and after passing this threshold the dynamics will be restricted to the interval $[1-d, 1]$ where $f_{\mathrm{F}}(x)$ is negative. In this interval the densities coincide with the densities calculated for $d > 1$.

The case $d = 1$ differs from the other cases in that the linear term in $f_{\mathrm{F}}(x)$ vanishes. For this reason, one term of the probability density becomes an exponential function:

$$\rho_{\mathrm{R}}^{\infty}(x) \propto x^{-(k_{\mathrm{RF}}+1)}(1-x)^{k_{\mathrm{RF}}-1}\exp(-k_{\mathrm{FR}}/x), \tag{2.8}$$

$$\rho_{\mathrm{F}}^{\infty}(x) \propto x^{-(k_{\mathrm{RF}}+2)}(1-x)^{k_{\mathrm{RF}}}\exp(-k_{\mathrm{FR}}/x). \tag{2.9}$$

The probability densities (2.6) and (2.7) enable us to quantify the levels x_{R} and x_{F} that the prey reaches while the predator is in the resting state R or the feeding state F, respectively. In Appendix B we derive the expected values $\mathbb{E}[x_{\mathrm{R}}]$ and $\mathbb{E}[x_{\mathrm{F}}]$ for the prey population depending on the predator being in the resting or the feeding state:

$$\mathbb{E}[x_{\mathrm{R}}] = \frac{C}{p_{\mathrm{R}}^{\infty}}(d-1)^{-a_{\mathrm{R}}}\,\mathrm{B}\left(b_{\mathrm{R}}+1, c_{\mathrm{R}}-b_{\mathrm{R}}\right){}_2F_1\left(a_{\mathrm{R}}, b_{\mathrm{R}}+1; c_{\mathrm{R}}+1, \frac{1}{1-d}\right) \tag{2.10}$$

$$\mathbb{E}[x_{\mathrm{F}}] = \frac{C}{p_{\mathrm{F}}^{\infty}}(d-1)^{-a_{\mathrm{F}}}\,\mathrm{B}\left(b_{\mathrm{F}}+1, c_{\mathrm{F}}-b_{\mathrm{F}}\right){}_2F_1\left(a_{\mathrm{F}}, b_{\mathrm{F}}+1; c_{\mathrm{F}}+1, \frac{1}{1-d}\right) \tag{2.11}$$

with $a_{\mathrm{R}} = \frac{k_{\mathrm{FR}}}{d-1}$, $b_{\mathrm{R}} = \frac{k_{\mathrm{FR}}}{d-1} - k_{\mathrm{RF}}$ and $c_{\mathrm{R}} = \frac{k_{\mathrm{FR}}}{d-1}$ as well as $a_{\mathrm{F}} = \frac{k_{\mathrm{FR}}}{d-1}+1$, $b_{\mathrm{F}} = \frac{k_{\mathrm{FR}}}{d-1} - k_{\mathrm{RF}}$ and $c_{\mathrm{F}} = \frac{k_{\mathrm{FR}}}{d-1}+1$. The normalisation constant C is derived in Appendix A.2, B is the beta function and ${}_2F_1$ the hypergeometric function.

Analogously to (2.10), (2.11) we calculate

$$\mathbb{E}[x_{\mathrm{R}}^2] = \frac{C}{p_{\mathrm{R}}^{\infty}}(d-1)^{-a_{\mathrm{R}}}\,\mathrm{B}\left(b_{\mathrm{R}}+2, c_{\mathrm{R}}-b_{\mathrm{R}}\right){}_2F_1\left(a_{\mathrm{R}}, b_{\mathrm{R}}+2; c_{\mathrm{R}}+2, \frac{1}{1-d}\right) \tag{2.12}$$

$$\mathbb{E}[x_{\mathrm{F}}^2] = \frac{C}{p_{\mathrm{F}}^{\infty}}(d-1)^{-a_{\mathrm{F}}}\,\mathrm{B}\left(b_{\mathrm{F}}+2, c_{\mathrm{F}}-b_{\mathrm{F}}\right){}_2F_1\left(a_{\mathrm{F}}, b_{\mathrm{F}}+2; c_{\mathrm{F}}+2, \frac{1}{1-d}\right) \tag{2.13}$$

so that we can find the variances $\mathrm{Var}[x_\mathrm{R}]$ and $\mathrm{Var}[x_\mathrm{F}]$ (and from these the standard deviations $\mathrm{SD}(x_\mathrm{R})$ and $\mathrm{SD}(x_\mathrm{F})$) using the formula $\mathrm{Var}(X) = \mathbb{E}[X^2] - \mathbb{E}[X]^2$:

$$\mathrm{Var}(x_\mathrm{R}) = \mathbb{E}[x_\mathrm{R}^2] - \mathbb{E}[x_\mathrm{R}]^2, \quad \mathrm{SD}(x_\mathrm{R}) = \sqrt{\mathrm{Var}(x_\mathrm{R})}, \tag{2.14}$$

$$\mathrm{Var}(x_\mathrm{F}) = \mathbb{E}[x_\mathrm{F}^2] - \mathbb{E}[x_\mathrm{F}]^2, \quad \mathrm{SD}(x_\mathrm{F}) = \sqrt{\mathrm{Var}(x_\mathrm{F})}. \tag{2.15}$$

3. Results

3.1. *Dynamics for fast and slow rates k_{RF} and k_{FR}*

We run the model (2.1), (2.2) for different choices for the transition rates $k_\mathrm{RF}, k_\mathrm{FR}$ which describe how frequently the predator switches between the resting state R and the feeding state F, see Fig. 2.

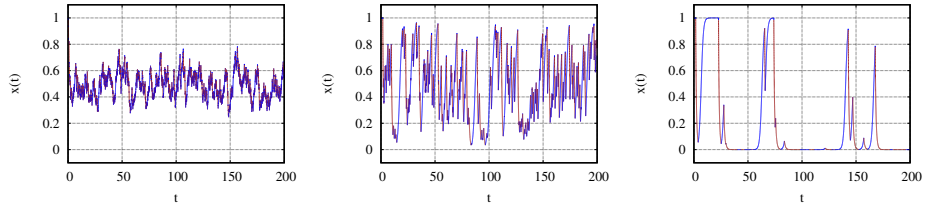

(a) $k_\mathrm{RF} = 10, k_\mathrm{FR} = 30$ (b) $k_\mathrm{RF} = 1, k_\mathrm{FR} = 3$ (c) $k_\mathrm{RF} = 0.1, k_\mathrm{FR} = 0.3$

Fig. 2: The dynamics of the model (2.1), (2.2) strongly depends on how quickly the individual switches between the resting state R and the feeding state F. We show realisations for the transition rates k_RF and k_FR chosen at three different orders of magnitude (a) "fast" ($k_\mathrm{RF} = 10, k_\mathrm{FR} = 30$), (b) "intermediate" ($k_\mathrm{RF} = 1, k_\mathrm{FR} = 3$) and (c) "slow" ($k_\mathrm{RF} = 0.1, k_\mathrm{FR} = 0.3$). In each plot, we have displayed the graph of the prey level x over time in blue if the predator is in the resting state R and in brown if it is in the feeding state F.

For each of the simulations we parameterise the model with $d = 2$ and start at the carrying capacity, i.e. at $x_0 = 1$. For $k_\mathrm{RF} = 10, k_\mathrm{FR} = 30$, see Fig. 2a, the population of the prey x decreases until it varies around an average level of approximately $x^* \approx 0.5$. If both transition rates are decreased by a factor of 10 the variation of x increases considerably—for $k_\mathrm{RF} = 1, k_\mathrm{FR} = 3$ it varies nearly across the complete range between 0 and 1. Decreasing the transition rates by another order of magnitude—to $k_\mathrm{RF} = 0.1, k_\mathrm{FR} = 0.3$—changes the appearance of the solutions considerably, see Fig. 2c. Instead of rapid variations around a stochastic "steady state", for these parameters, periods of prey growth and decline alternate, which gives the impression of stochastic oscillatory dynamics.

Due to stochasticity, these "oscillations" are not regular—in Fig. 2c, the periods during which the prey population is near extinction show considerable variations in duration. This becomes even more apparent in Fig. 3.

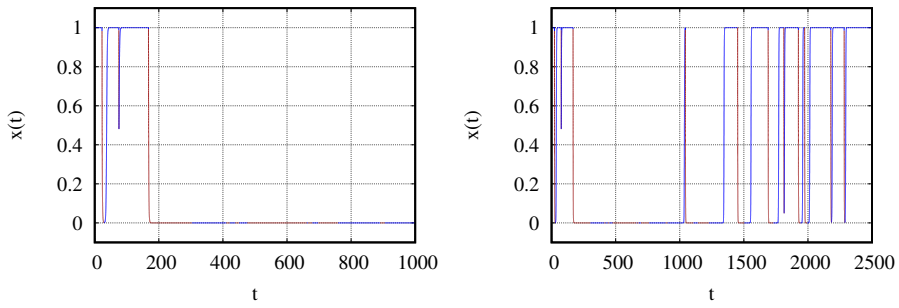

(a) Simulation until $t = 1,000$ (b) Simulation until $t = 2,500$

Fig. 3: (a) For very small values of the rates, $k_{\mathrm{RF}} = 0.01$, $k_{\mathrm{FR}} = 0.03$, the population x might be reduced to very low densities. (b) However, due to the instability of the extinction state $x^{\infty}_{\mathrm{ext}} = 0$ of the logistic model, the population will never go extinct.

If we simulate the model with $k_{\mathrm{RF}} = 0.01, k_{\mathrm{FR}} = 0.03$ over a much larger time interval—for 1,000 time units instead of 200 as in our previous simulations (Fig. 2)—the realisation shown in Fig. 3a gives the impression that the prey population has gone extinct. However, due to the instability of the stationary solution x^{∞}_0, it is clear that this is not possible. Indeed, looking at Fig. 3b we see that only shortly after $t = 1,000$ the prey x shows a sudden outburst. In the remaining time interval between 1,000 and 2,500, the population "oscillates" much more rapidly than between 0 and 1,000.

This, despite the simplicity of the model, surprisingly complex behaviour, becomes even more difficult to analyse due to stochasticity—no two "realisations" of the model will be the same.

3.2. *The probability densities $\rho_R(t;x)$, $\rho_F(t;x)$ and $\rho^{\infty}_R(x)$, $\rho^{\infty}_F(x)$*

For this reason we now take advantage of the fact that we can calculate the probability densities for the states R and F of a piece-wise deterministic Markov process (PDMP) over time. Let us first consider the probability distribution of the two-state Markov model (2.1) for switching between R and F (not coupled, yet, to the model (2.2)). Fig. 4a shows, for the parameters $k_{\mathrm{RF}} = 10, k_{\mathrm{FR}} = 30$, how the probabilities $p_{\mathrm{R}}(t)$ and $p_{\mathrm{F}}(t)$ of being in the states R or F, respectively, develop over time, assuming that we started in state R, i.e. we set the probability of $S = \mathrm{R}$ to 1 for $t = 0$ so that $\mathbf{p}^0_{\mathrm{RF}} = (p^0_{\mathrm{R}}, p^0_{\mathrm{F}}) = (1, 0)$. We observe that $\mathbf{p}_{\mathrm{RF}}(t)$ rapidly tends to the stationary distribution $\mathbf{p}^{\infty}_{\mathrm{RF}} = \left(\frac{k_{\mathrm{FR}}}{k_{\mathrm{RF}}+k_{\mathrm{FR}}}, \frac{k_{\mathrm{RF}}}{k_{\mathrm{RF}}+k_{\mathrm{FR}}}\right) = (3/4, 1/4)$. This implies that, on average, the predator spends three times as much time in the resting state than in the feeding state. This holds, indeed, for all parameter sets considered in Figs. 2 and 3 because for each of these parameter sets we have $k_{\mathrm{FR}} = 3k_{\mathrm{RF}}$.

After coupling the Markov model (2.1) to the differential equation (2.2), the

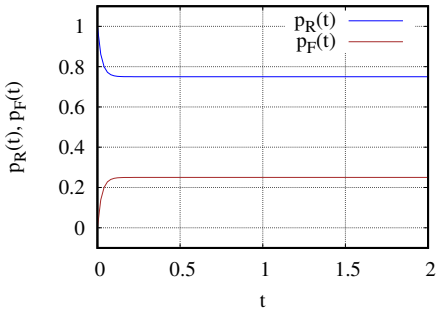

(a) $\mathbf{p}_{\mathrm{RF}}(t)$ according to (2.1)

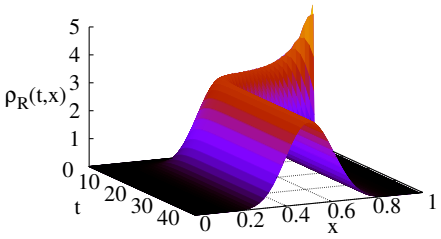

(b) $\rho_{\mathrm{R}}(t;x)$ according to (2.3)

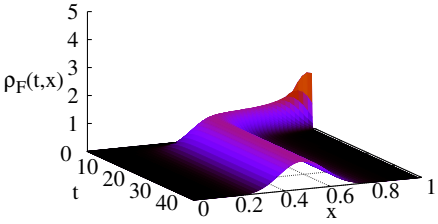

(c) $\rho_{\mathrm{F}}(t;x)$ according to (2.3)

Fig. 4: The probability density functions $\rho_{\mathrm{R}}(t;x)$ and $\rho_{\mathrm{F}}(t;x)$ enable us to investigate the probability density of the individual over the states R and F depending on the prey density x.

state space of the resulting PDMP not only consists of R and F but also the continuous variable x, the size of the prey population. Due to the dependency on a continuous variable, rather than probabilities p_{R}, p_{F}, we obtain probability densities $\rho_{\mathrm{R}}(t;x)$ and $\rho_{\mathrm{F}}(t;x)$ which can be calculated by solving the advection equation (2.3). Here, $\boldsymbol{\rho}_{\mathrm{RF}}(0;x) = \boldsymbol{\rho}^0_{\mathrm{RF}}(x)$ have been initialised such that all support of $\rho^0_{\mathrm{R}}(x)$ is concentrated close to $x = 1$ and $\rho^0_{\mathrm{F}}(x) = 0$. This is analogous to the initial condition $p^0_{\mathrm{R}} = 1, p^0_{\mathrm{F}} = 0$ chosen for (2.1) shown in Fig. 4a—the system starts in state R and at the carrying capacity $x = 0$. Figs. 4b and 4c illustrate how the probability densities $\rho_{\mathrm{R}}(t;x)$ and $\rho_{\mathrm{F}}(t;x)$ develop in time.

Although ρ_{F} was initialised with zero at $t = 0$, the density rapidly increases. This is because due to the relatively large values for the rates k_{RF} and k_{FR} of the infinitesimal generator $\mathbf{Q}_{\mathrm{RF}}$ it is likely that the predator will quickly switch from the resting state R to the feeding state F.

Both densities $\rho_{\mathrm{R}}(t;x)$ and $\rho_{\mathrm{F}}(t;x)$ move towards lower prey densities x until they converge to stable distributions $\rho^\infty_{\mathrm{R}}(x)$ and $\rho^\infty_{\mathrm{F}}(x)$, both centered at approximately $x = 0.5$. This is consistent with the simulations shown in Fig. 2a—the prey population is found to be close to $x = 0.5$ independent of the predator being in the resting state R or the feeding state F or, in other words: the system has reached a stochastic steady state. By calculating the areas under the curves of

the stationary distributions $\rho_{\mathrm{R}}^{\infty}$ and $\rho_{\mathrm{F}}^{\infty}$, we can relate these results to the stationary probabilities $p_{\mathrm{R}}^{\infty} = 3/4$ and $p_{\mathrm{F}}^{\infty} = 1/4$ shown in Fig. 4a. Indeed, we can verify that $p_{\mathrm{R}}^{\infty} = \int_0^1 \rho_{\mathrm{R}}^{\infty}(x)dx = 3/4$ and $p_{\mathrm{F}}^{\infty} = \int_0^1 \rho_{\mathrm{F}}^{\infty}(x)dx = 1/4$ and the areas under the curves $\rho_{\mathrm{R}}(t = 40, x)$ and $\rho_{\mathrm{F}}(t = 40, x)$ obtained for $t = 40$ seem to roughly differ by a factor of 3, consistent with the results obtained for p_{R}^{∞} and p_{F}^{∞} from Fig. 4a—also, compare with the steady-state densities $\rho_{\mathrm{R}}^{\infty}(x)$ and $\rho_{\mathrm{F}}^{\infty}(x)$ shown in Fig. 5a.

Figs. 4b and 4c show that the dynamics is characterised by a transient phase which rapidly converges to stationary densities $\rho_{\mathrm{R}}^{\infty}(x)$, $\rho_{\mathrm{F}}^{\infty}(x)$. Due to the rapid transient which influences the dynamics of x only for a relatively brief initial phase, the stationary densities are much more interesting to us. How do the densities $\rho_{\mathrm{R}}^{\infty}(x)$ and $\rho_{\mathrm{F}}^{\infty}(x)$ relate to the dynamics of x? From Fig. 5a we can get a more rigorous idea what it means that the prey x has reached a stochastic steady state in Fig. 2a. As explained above, both densities $\rho_{\mathrm{R}}^{\infty}(x)$ and $\rho_{\mathrm{F}}^{\infty}(x)$ are centered roughly around $x \approx 0.5$. This means that we can "expect" to find the population x near values of 0.5—we will, actually, be able to make this "expectation" more rigorous when we calculate the expected values below. By considering the support of both densities, $\mathrm{supp}(\rho_{\mathrm{R}}^{\infty}) \approx \mathrm{supp}(\rho_{\mathrm{F}}^{\infty}) \approx [0.25, 0.8]$, we get a clear idea how large the variation around the stochastic steady state is—indeed, Fig. 2a shows that x varies over the range of the interval $[0.25, 0.8]$.

When we compare the solutions shown in Fig. 2a with Fig. 2b where the parameters $k_{\mathrm{FR}} = 1, k_{\mathrm{RF}} = 3$ ensure that the switching between resting and feeding is an order of magnitude slower, the main difference is the much larger variability of x which now seems to vary across the whole range $[0, 1]$. This is again clearly indicated by the stationary densities shown in Fig. 5b—the support of both now ranges across the complete interval $[0, 1]$ and both distributions are a lot more wide-spread which appropriately describes the large variations seen in Fig. 2b. In contrast to the results for faster switching presented previously and the model behaviour for slower switching between resting and feeding which will be described next, the dynamics is characterised by considerable stochastic variations that make it more difficult than for the other parameter sets to discern a clear pattern or constrain the population dynamics to a subset of $[0, 1]$.

As we decrease k_{RF} and k_{FR} further (see Figures 5c and 5d), slowing down the dynamics of switching between resting and feeding to an even greater extent, the appearance of $\rho_{\mathrm{R}}^{\infty}(x)$ and $\rho_{\mathrm{F}}^{\infty}(x)$ changes drastically. Because $\rho_{\mathrm{R}}^{\infty}(x)$ and $\rho_{\mathrm{F}}^{\infty}(x)$ are concentrated at the boundaries of the interval $x = 0$ and $x = 1$, in order to appropriately visualise the distributions, the densities are shown in a bi-logarithmic plot. Both $\rho_{\mathrm{R}}^{\infty}(x)$ and $\rho_{\mathrm{F}}^{\infty}(x)$ have low values for most of the interval $[0, 1]$ but very steeply increase to large values for $x \to 0$. In contrast, as we tend to $x = 1$, the density $\rho_{\mathrm{F}}^{\infty}(x)$ tends to zero whereas $\rho_{\mathrm{R}}^{\infty}(x)$ tends to large values. This means that $\rho_{\mathrm{F}}^{\infty}(x)$ is unimodal and has a sharp peak at $x = 0$ whereas $\rho_{\mathrm{R}}^{\infty}(x)$ is bimodal and tends to large values for both $x \to 0$ and $x \to 1$. Comparing Figures 5c and 5d we notice that the densities for $k_{\mathrm{RF}} = 0.1, k_{\mathrm{FR}} = 0.3$ and $k_{\mathrm{RF}} = 0.01, k_{\mathrm{FR}} = 0.03$ appear qualitatively similar—both densities $\rho_{\mathrm{R}}^{\infty}(x)$ and $\rho_{\mathrm{F}}^{\infty}(x)$ for $k_{\mathrm{RF}} = 0.01, k_{\mathrm{FR}} = 0.03$

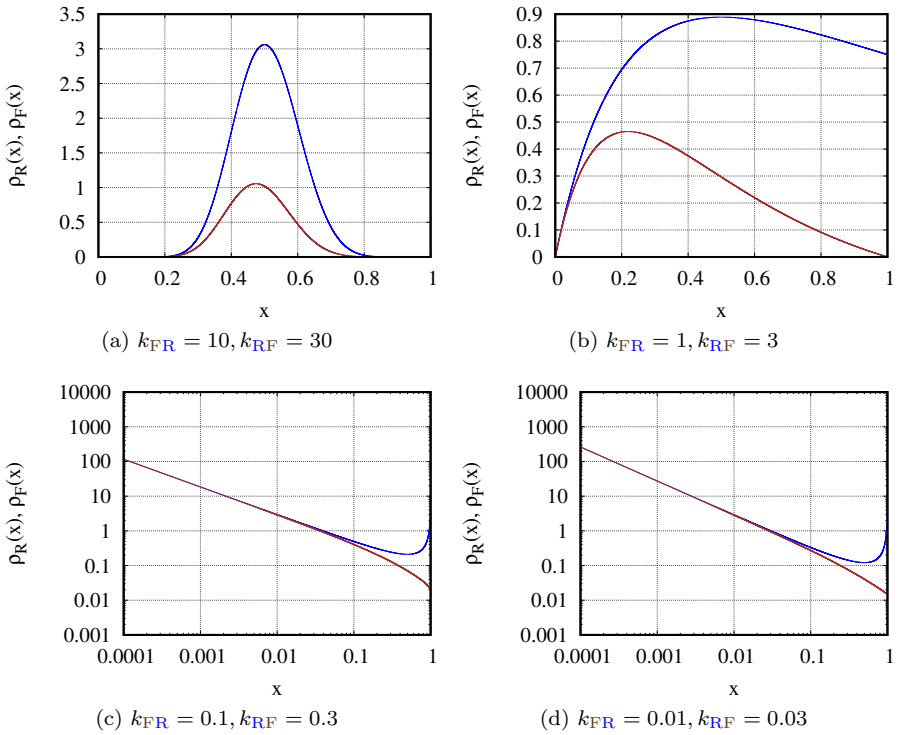

(a) $k_{\mathrm{FR}} = 10, k_{\mathrm{RF}} = 30$ (b) $k_{\mathrm{FR}} = 1, k_{\mathrm{RF}} = 3$

(c) $k_{\mathrm{FR}} = 0.1, k_{\mathrm{RF}} = 0.3$ (d) $k_{\mathrm{FR}} = 0.01, k_{\mathrm{RF}} = 0.03$

Fig. 5: Steady-state PDFs $\rho_{\mathrm{R}}^{\infty}(x)$ and $\rho_{\mathrm{F}}^{\infty}(x)$ calculated according to (2.6), (2.7). (a) For the fast transition rates $k_{\mathrm{RF}} = 10$, $k_{\mathrm{FR}} = 30$, $\rho_{\mathrm{R}}^{\infty}(x)$ and $\rho_{\mathrm{F}}^{\infty}(x)$ are both relatively narrow distributions centered around $x \approx 0.5$. (b) For $k_{\mathrm{RF}} = 1$, $k_{\mathrm{FR}} = 3$, at the same order of magnitude as the prey growth rate (which is scaled to unity), the support of both probability densities ranges over the whole interval $[0, 1]$ which implies that both in the resting as well as in the feeding state the model shows a lot more fluctuations. (c) and (d) For small transition rates, $k_{\mathrm{RF}} = 0.1$ and 0.01 as well as $k_{\mathrm{RF}} = 0.3$ and 0.03, $\rho_{\mathrm{F}}^{\infty}$ diverges for $x \to 0$ while tending to zero for $x \to 1$, indicating that the prey population most likely has low levels when the predator is in the feeding state F. In contrast, $\rho_{\mathrm{R}}^{\infty}$ tends to infinity for both $x \to 0$ and $x \to 1$. This is due to the fact that when the predator enters the resting state R, the prey is most likely close to zero because the predator typically has spent a long time in the feeding state F reducing x to very small values. Because the predator is then expected to spend a long time in the resting state R, not feeding on the prey, the prey population x will likely grow until it reaches the carrying capacity which is 1 and spend a considerable amount of time in this state before the predator again switches to the feeding state F.

seem to be approximately half of the densities for $k_{\mathrm{RF}} = 0.1, k_{\mathrm{FR}} = 0.3$. However, because in both cases we must have $\int_0^1 \rho_{\mathrm{R}}^{\infty}(x) + \rho_{\mathrm{F}}^{\infty}(x)dx = 1$ this shows that for

$k_{\mathrm{RF}} = 0.01, k_{\mathrm{FR}} = 0.03$ both $\rho_{\mathrm{R}}^{\infty}(x)$ and $\rho_{\mathrm{F}}^{\infty}(x)$ must increase even more sharply for very small values of x, so that both distributions are even more concentrated near $x = 0$. This means that if the prey level x is high, the predator is most likely to be found in the resting state R which is not very surprising. But, interestingly, for small prey levels x, the likelihoods of finding the predator in the feeding state F as well as in the resting state R are both high. The reason for this becomes clearer when considering the dynamics for $k_{\mathrm{RF}} = 0.01, k_{\mathrm{FR}} = 0.03$ (Fig. 3b). Whenever the predator switches to the feeding state F, indicated by the brown arcs of the curve, the prey density rapidly decreases, quickly reaching prey levels x close to zero. Because it typically takes some time before the predator stops feeding by switching back to the resting state R, the predator will most likely spend some time near $x = 0$. In Fig. 3b examples for this behaviour can, for example, be seen at $t \approx 200$, slightly above 1,000, close to 1,500 etc. Crucially, if the predator switches to F if the prey level x is already at a low level, the prey population will, of course, remain small—in Fig. 3b examples for this can be found in the interval $t \in [150, 1000]$. If, on the contrary, the predator enters the resting state R when the prey density x is low, the prey level will remain at a low level for a while before it rapidly increases—the reason for this is that logistic growth is initially slow for low population densities before it rapidly accelerates as the population increases and quickly reaches the carrying capacity $x = 1$. As can be seen in Fig. 3b, after having reached the carrying capacity $x = 1$, the predator usually remains in the resting state R for some time which is the reason that the distribution $\rho_{\mathrm{R}}^{\infty}(x)$ sharply increases for $x \to 1$. Because, as can be seen in Fig. 3b, the solution $x(t)$ mostly alternates between $x \approx 0$ and $x \approx 1$ and spends very little time at intermediate prey levels, both densities $\rho_{\mathrm{R}}^{\infty}(x)$ and $\rho_{\mathrm{F}}^{\infty}(x)$ have very low values apart from the boundaries of the interval $[0, 1]$.

Due to the slower dynamics, the Markov model $\mathbf{Q}_{\mathrm{RF}}$ spends more time in either of the two states so that the solutions of the model (2.2) develop, for considerably long time intervals, along the two branches defined for the resting state R and the feeding state F. Looking at Fig. 2c, it is now much more apparent that the dynamics shown is, in fact, pieced together from arcs of the form shown in Figs. 1c and 1d. These characteristics are amplified further in Fig. 3 where it even appears—between $t \approx 200$ and $t \approx 1,000$—that the prey has gone extinct.

These characteristics of the dynamics can also be seen by considering the expected values $\mathbb{E}[x_{\mathrm{R}}]$ and $\mathbb{E}[x_{\mathrm{F}}]$, see Fig 6.

3.3. *Extensions of the model*

So far, we have developed a model that, despite its surprisingly rich dynamics, seems too simplistic to be interesting. The predator behaves in the same way, independent if a small or a large amount of prey is present in the environment, and it is unaffected by how much prey it manages to consume. In predator-prey models based on differential equations the functional response describes how the predator adjusts its behaviour to the current prey population. In section 3.3.1 we will extend the model

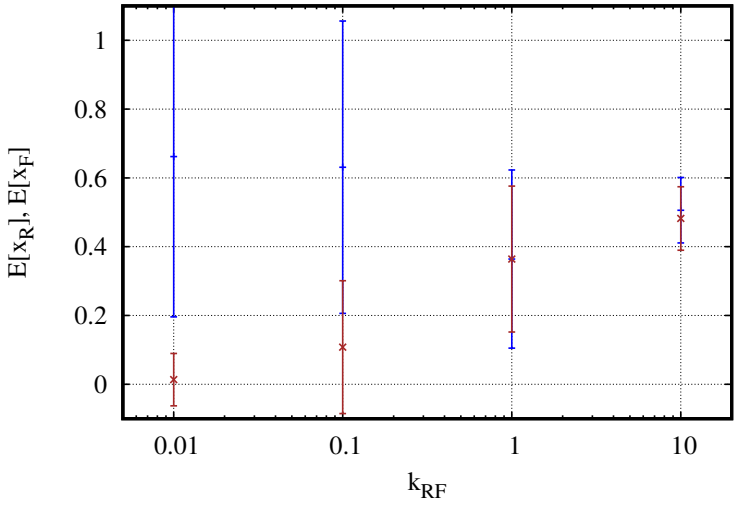

Fig. 6: Dependency of the expected values $\mathbb{E}[x_{\mathrm{R}}]$ and $\mathbb{E}[x_{\mathrm{F}}]$ with error bars one standard deviation long, $\mathrm{SD}(x_{\mathrm{R}})$ or $\mathrm{SD}(x_{\mathrm{F}})$, on the transition rate k_{RF} plotted on a logarithmic scale. Note that for the parameter sets considered here we always have $k_{\mathrm{FR}} = 3k_{\mathrm{RF}}$. On the right of the plot, for fast transition rates, $k_{\mathrm{FR}} = 10$, $k_{\mathrm{FR}} = 30$, the expected values are close to $x = 0.5$ with small standard deviations. For $k_{\mathrm{FR}} = 1$, $k_{\mathrm{FR}} = 3$ both expected values decrease and the standard deviations increase considerably due to the strong fluctuations observed for these parameter values. For slow rates, $k_{\mathrm{FR}} = 0.1$, $k_{\mathrm{FR}} = 0.3$ and $k_{\mathrm{FR}} = 0.01$, $k_{\mathrm{FR}} = 0.03$, $\mathbb{E}[x_{\mathrm{R}}]$ and $\mathbb{E}[x_{\mathrm{F}}]$ drift apart from each other—$\mathbb{E}[x_{\mathrm{F}}]$ attains small values close to zero with low standard deviations $\mathrm{SD}(x_{\mathrm{F}})$ indicating that while in the feeding state F the predator drives the prey nearly to extinction. At the same time, $\mathbb{E}[x_{\mathrm{R}}]$ as well as the standard deviation $\mathrm{SD}(x_{\mathrm{R}})$ increase. The reason for this is that for slow transition rates, the predator usually enters the resting state R when the prey population x is at very low values but remains in this state for long enough that the prey population recovers and spends a relatively long time close to the carrying capacity $x = 1$.

by introducing prey-dependent rates $k_{\mathrm{RF}}(x)$ and $k_{\mathrm{FR}}(x)$. A related unrealistic feature of our original model is that the amount of prey consumed has no effect on the well-being of the predator. We address this issue by adding an energy variable E that is depleted while the predator is in the resting state R and replenished while it is in the feeding state F (Section 3.3.2). Finally, so far we have only considered a single predator, in Section 3.3.3 we will explain how the model can be extended to

multiple predators.

3.3.1. *Adaptive predators*

So far, we have considered constant transition rates k_{RF} and k_{FR} which means that the predator alternates between resting and feeding independent of the amount of prey x present. We will now consider a variant of the model where the predator adjusts the transitions between resting and feeding based on the amount of prey x found in the environment:

$$k_{\mathrm{RF}}(x) = \tilde{k}_{\mathrm{RF}} \cdot x, \tag{3.1}$$

$$k_{\mathrm{FR}}(x) = \tilde{k}_{\mathrm{FR}} \cdot (1 - x), \; x \in [0, 1]. \tag{3.2}$$

The dependency of the rates $k_{\mathrm{RF}}(x)$, $k_{\mathrm{FR}}(x)$ described in (3.1), (3.2) represents a predator which adjusts its behaviour to the availability of food i.e. it preferably moves to the feeding state F for large abundance and tends to the resting state R for small abundance of prey x. For the example shown in Fig. 7 we find only minor differences when comparing the dynamics of the model with constant transition rates $k_{\mathrm{FR}} = 0.1, k_{\mathrm{RF}} = 0.2$ and the adaptive model (3.2), (3.1), with $\tilde{k}_{\mathrm{RF}} = 0.1, \tilde{k}_{\mathrm{FR}} = 0.2$.

3.3.2. *Physiological states: An energy level for the predator*

So far, our model does not account for the fact that a predator can only survive if it consumes a sufficient amount of prey x. This can be accounted for by introducing a physiological state that represents the energy level E of the predator:

$$\frac{dE}{dt} = \begin{cases} -\kappa E, & S = \mathrm{R} \\ e\, d\, x - \kappa E, & S = \mathrm{F} \end{cases}. \tag{3.3}$$

The differential equation (3.3) for the energy level E is based on the assumption that due to metabolism, energy is continuously consumed at a rate κ. However, while the predator is feeding, energy can be replenished at a rate edx proportional to the amount of prey consumed dx. Introducing a physiological state variable such as E opens up a wide range of possibilities for a more realistic representation of a predator:

- An energy-dependent rate k_{FR} could represent "exhaustion" by increasing the rate to the resting state for low energy levels E.
- Energy-dependency of the rate k_{RF} could be used for representing "hunger"—the transition rate to the feeding state would increase with decreasing energy levels E.
- Decreasing the catch rate d with declining energy levels could account for the fact that the hunting success might decrease due to "weakness".

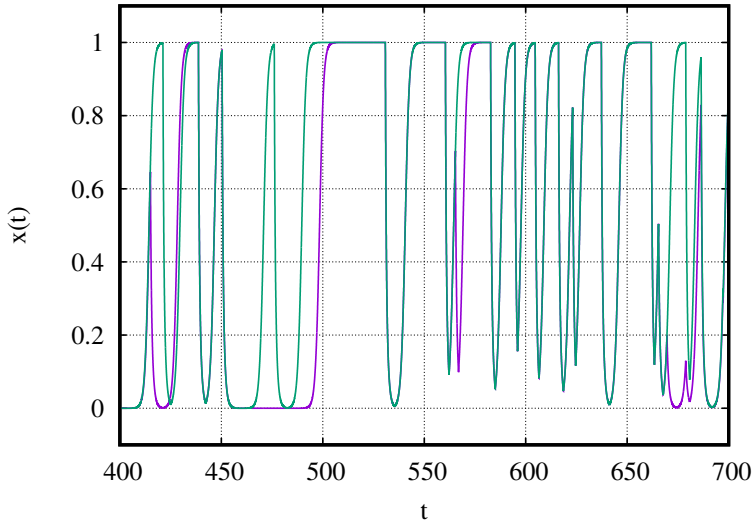

Fig. 7: Comparison of a predator that alternates between the resting state R and feeding state F at constant transition rates $k_{\mathrm{FR}} = 0.1, k_{\mathrm{RF}} = 0.2$ (plotted in purple) with a predator that adapts resting and feeding to the abundance of prey x according to (3.1), (3.2) (plotted in green) with $\tilde{k}_{\mathrm{RF}} = 0.1, \tilde{k}_{\mathrm{FR}} = 0.2$. The prey population x was simulated for both models using the same realisation of random numbers generated by choosing the same seed for the random number generator. Interestingly, we find only minor differences between the prey-independent and the adaptive predator.

Moreover, getting too close to $E = 0$ could be taken as a condition for loss of life. Despite the possibly considerable additional complexity due to this physiological state, the resulting model can still be analysed using the methods explained in this study—the probability densities will depend on the additional variable E i.e. $\rho_{\mathrm{R}}(t; x, E)$ and $\rho_{\mathrm{F}}(t; x, E)$. We present an example for constant transition rates $k_{\mathrm{RF}} = 0.1$, $k_{\mathrm{FR}} = 0.3$, $d = 2$, $e = 1$, $\kappa = 0.1$, see Figure 8.

3.3.3. *Multiple predators*

So far we have only considered a single predator feeding on the prey x. We will briefly illustrate how multiple predators can be represented in our model. Although it would, of course, be possible to consider separate Markov models for each individual predator, it is advantageous to combine the infinitesimal generators of each

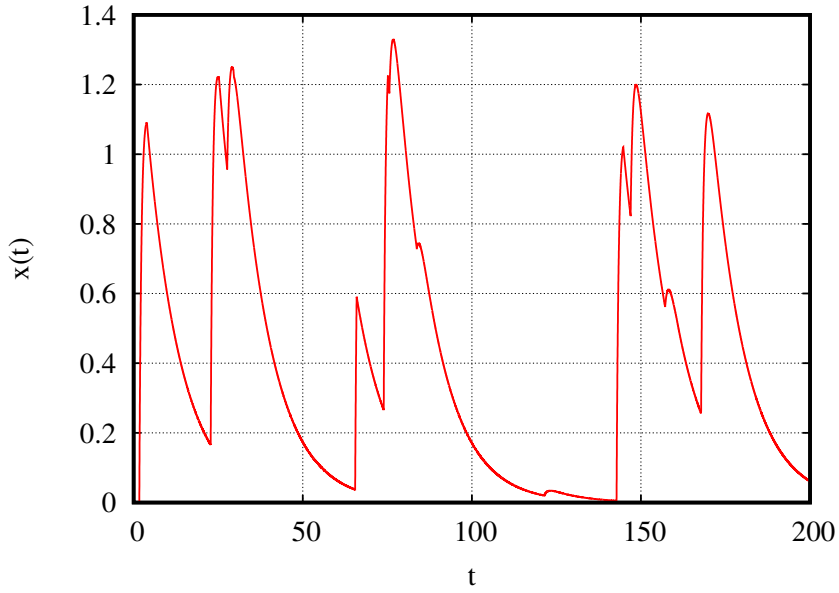

Fig. 8: Introducing an energy level E for the predator as an example for a physiological state, see (3.3). It is assumed that the predator needs energy for homeostasis, so the energy level E of the predator continuously decreases. When the predator consumes prey the energy level increases depending on the amount of prey consumed. The plot shows the time course of E calculated according to the model (3.3). In future work we will explore coupling of the energy level to the feeding and resting behaviour of the predator.

individual predator to a common infinitesimal generator that simultaneously represents the states of all individuals. This enables us to continue using the framework of PDMPs in the same way as previously—mathematically the only difference between a PDMP representing a single predator and one representing multiple predators is that the state space of the Markov model is augmented. Here, we will restrict ourselves to the case of two identical stochastically independent predators. Increasing the number of predators is straightforward and we refer to various complementary approaches for constructing Markov models for multiple individuals with different forms of dependency.

Via an operation known as the Kronecker sum '$\oplus$' the infinitesimal generators of two stochastically independent Markov models are combined to form a generator that simultaneously describes the dynamics of both models

$$\begin{aligned}\mathbf{Q}_{\mathrm{RFRF}} &= \mathbf{Q}_{\mathrm{RF}} \oplus \mathbf{Q}_{\mathrm{RF}} \\ &= \mathbf{Q}_{\mathrm{RF}} \otimes \mathbf{id}_n + \mathbf{id}_n \otimes \mathbf{Q}_{\mathrm{RF}} \\ &= \begin{pmatrix} -2k_{\mathrm{RF}} & k_{\mathrm{RF}} & k_{\mathrm{RF}} & 0 \\ k_{\mathrm{FR}} & -k_{\mathrm{FR}} - k_{\mathrm{RF}} & 0 & k_{\mathrm{RF}} \\ k_{\mathrm{FR}} & 0 & -k_{\mathrm{FR}} - k_{\mathrm{RF}} & k_{\mathrm{RF}} \\ 0 & k_{\mathrm{FR}} & k_{\mathrm{FR}} & -2k_{\mathrm{FR}} \end{pmatrix},\end{aligned} \tag{3.4}$$

where '$\otimes$' stands for the Kronecker product i.e. the tensor product for matrices. The result of the operation carried out on the two copies of the model with generator $\mathbf{Q}_{\mathrm{RF}}$ described in (3.4) is illustrated in the diagram shown in Fig. 9a. First, we observe that the state space of the resulting model is the Cartesian product $\mathcal{S} \times \mathcal{S} =: \mathcal{S}^2$ of the state space $\mathcal{S} = \{\mathrm{R}, \mathrm{F}\}$ of the individual models. In the pairs (R, R), (R, F), (F, R) and $(\mathrm{F}, \mathrm{F}) \in \mathcal{S}^2$, the first component contains the state of the first whereas the second component contains the states of the second of the two models. Second, within each of the states of the state space $\mathcal{S}^2$, a transition to a new state is made if one of the two states changes. So, for example, in the topmost state (F, R) in the diagram Fig. 9a either the first state can change from F to R via the transition rate k_{FR} reaching (R, R) or instead—due to R transitioning to F via k_{RF}—the model can switch to (F, F). In contrast, moving directly from (F, R) to (R, F) is not possible because this would involve a simultaneous transition of both states.

A slightly simplified representation of this model based on three rather than fours states can be obtained by identifying the two states (R, F) and (F, R) resulting in a model representation that accounts for the number of models that are in the feeding state F (Fig. 9b) via the states F_0, F_1,F_2. The infinitesimal generator can be calculated from (3.4):

$$\mathbf{Q}_{\mathrm{RFRF}} = \begin{pmatrix} -2k_{\mathrm{RF}} & 2k_{\mathrm{RF}} & 0 \\ k_{\mathrm{FR}} & -k_{\mathrm{FR}} - k_{\mathrm{RF}} & k_{\mathrm{RF}} \\ 0 & 2k_{\mathrm{FR}} & -2k_{\mathrm{FR}} \end{pmatrix}. \tag{3.5}$$

As with the one-predator model, the model is simulated by coupling the generator, (3.4) or, analogously, (3.5), to the differential equation (2.2). The total grazing rate is found by multiplying d with the number n_{F} of predators that are in the feeding state F at a particular moment in time. One realisation of simulating the model for two predators with $k_{\mathrm{RF}} = 0.01$, $k_{\mathrm{FR}} = 0.05$ and $d = 0.5$ is shown in Fig. 9c. It can be clearly seen how many predators are in the feeding state F (two, one or none). Note that choosing $d = 0.5$, when only one predator feeds on the prey population x the growth of the prey population is reduced which leads to a reduction of the carrying capacity from $x = 1$ to 0.5). For $d = 0.5$ only two predators feeding simultaneously can reduce the prey population to levels close to the (unstable) extinction state $x_{\mathrm{ext}} = 0$.

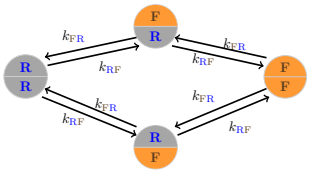

(a) Model for two predators

(b) Reduced two-predator model

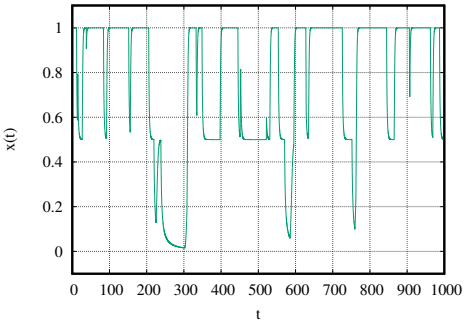

(c) Simulation

Fig. 9: Modelling two stochastically independent predators. In (a) we see the model structure obtained by combining two models $\mathbf{Q}_{\mathrm{RF}}$ with identical parameters via $\mathbf{Q}_{\mathrm{RFRF}} = \mathbf{Q}_{\mathrm{RF}} \oplus \mathbf{Q}_{\mathrm{RF}}$. This model structure can be simplified by identifying the two states (F, R) and (R, F). This leads to a model that only accounts for the number of models that are in state F. The model structure of this simplified model is shown in (b). In (c) we show results of simulating this model with parameters $k_{\mathrm{RF}} = 0.01$, $k_{\mathrm{FR}} = 0.05$, $d = 0.5$.

4. Discussion

We have shown, using a simple example, that piecewise-deterministic Markov processes (PDMPs), also known as hybrid stochastic systems, can be used for developing individual-based models (IBMs) that on the one hand offer a large amount of flexibility in the model design but on the other hand are amenable to systematic mathematical analysis. This enables us to investigate the behaviour of a model more efficiently and also has the potential to reveal some more general patterns than if we had to solely rely on extensive simulation studies.

Despite its simplicity, the model presented here, of a predator that intermittently feeds on a logistically growing prey population x by switching between a resting state R and a feeding state shows surprisingly rich dynamics. If the growth rate of the prey population is small in comparison with the rates at which the predator alternates between resting and feeding, the prey population fluctuates around a stochastic steady state below the carrying capacity. For transition rates k_{RF} and k_{FR} at the same order of magnitude as the prey growth rate the fluctuations increase. In fact, this is the parameter regime where the dynamics of the system is most difficult to predict, as the prey population seems to vary erratically across the whole range $[0, 1]$. If the predator behaviour switches significantly more slowly than the growth rate of the prey, the dynamics develops an oscillatory characteristic. This is a simple consequence of the fact that the time spent in either the resting

or the feeding state is long in comparison to the population dynamics of the prey population. If the prey population is at a low level close to zero, as the predator switches to the resting state R it will remain in this state for sufficiently long so that the prey population can x can grow close to its carrying capacity. As the prey remains close to the carrying capacity, eventually the predator will transition to the feeding state F and remain in this state for sufficiently long so that the prey population x decreases to a level close to zero. In summary, because the predator switches between resting state R and feeding state F much more slowly than the prey population x grows or declines according to the logistic growth model (2.2), the predator-prey dynamics is pieced together by arcs of the form shown in Fig. 1c and 1d. This results in oscillations which become increasingly sharper the slower the time scale of switching between the behavioural states of the predator is in comparison with the growth rate of the prey.

Until this point we have obtained a general qualitative impression of the predator-prey dynamics of our model. It is now natural to investigate quantitative aspects of the dynamics in more detail. For example, we might ask questions such as:

- If the prey reaches a stochastic steady state, what is the approximate level of this steady state? How strong do we expect the stochastic fluctuations to be?
- For which parameter ranges do we expect to see qualitatively different dynamics? For the model investigated in this study for which parameters do we expect to see ...
  - ... a stochastic steady state?
  - ... stochastic fluctuations?
  - ... oscillatory dynamics?

For our model based on PDMPs, these questions can all be answered by analysing the probability densities $\rho_{\mathrm{R}}^{\infty}(x)$ and $\rho_{\mathrm{F}}^{\infty}(x)$—computing the expected values $\mathbb{E}[x_{\mathrm{R}}]$ and $\mathbb{E}[x_{\mathrm{F}}]$ yields the stochastic steady state x whereas the fluctuations can be quantified by calculating the variance of the expected values. Parameter-dependent changes in the qualitative dynamics can be investigated by studying how the densities $\rho_{\mathrm{R}}^{\infty}(x)$ and $\rho_{\mathrm{F}}^{\infty}(x)$ respond to parameter changes as we have demonstrated in our analysis. We have deliberately chosen a model so simple that these densities as well derived quantities such as the expected values $\mathbb{E}[x_{\mathrm{R}}]$ and $\mathbb{E}[x_{\mathrm{F}}]$ can be calculated analytically. However, for more detailed models for which calculating the probability densities is intractable, the equations defining the densities $\rho_{\mathrm{R}}(t,x)$ and $\rho_{\mathrm{F}}(t,x)$ as well as the steady state densities $\rho_{\mathrm{R}}^{\infty}(x)$ and $\rho_{\mathrm{F}}^{\infty}(x)$ can be solved numerically using standard finite-difference methods.[44] Obtaining numerical solutions for the probability densities is in almost all cases much faster than running full stochastic simulations—these would also have to be repeated multiple times to approximate the probability densities. Analyses similar to what has been presented here can be carried out in the same way as presented here, no matter if

the probability densities were obtained In contrast, for an IBM based on a more flexible architecture, a mathematical framework for analysing the model behaviour is, at least initially, not available and the modeller has to investigate the model in a heuristic fashion.

We have also investigated the question if designing an IBM as a PDMP constrains the model architecture to an extent that the benefits of following an individual-based modelling approach are lost. We believe that our extensions of the model in several directions demonstrate that such concerns are unwarranted. We have demonstrated that by coupling the transition rates of the Markov model describing the predator to the prey population, adaptive behaviour can be introduced to the model (Section 3.3.1). We have shown that physiological states of the predator such as an energy level that depends on the prey consumed can be incorporated into the model via additional differential equations (Section 3.3.2). In our investigation of a model describing multiple predators we have only considered the simplest case of predators that are only interacting via the shared prey population (Section 3.3.3), however, various models that can be used for directly interacting individuals are available from the literature on interacting ion channels.[47–49]

Because in this study we have deliberately chosen a very simple model to illustrate how IBMs can be designed using PDMPs we would like to discuss the challenges of applying this approach for designing more realistic models. More detailed models will most likely have one or more of the following characteristics. They will...

(1) ... have (possibly many) more states to obtain a more realistic representation of individuals.
(2) ... account for (possibly many more) individuals than one or two, as considered here.
(3) ... be coupled to systems of differential equations that describe on the one hand populations that interact with the individuals described by the Markov models as well as on the other hand continuous states that account for states of the individuals such as the energy level introduced in section 3.3.2.

The main consequence of these challenges is—as already explained above—that the probability densities ρ_S for states S will typically have to be calculated numerically because analytical solutions are either not available or too cumbersome to be useful in practice. This is, in principle, not a restriction because the complete analysis presented here could easily have been carried out in the same way relying on numerical solutions.

However, by increasing the number of states, the approach presented here requires one to investigate a large number of probability densities ρ_S, which might make it difficult to obtain meaningful insights into the dynamics. We believe that one important method to address this is to take care that the state space of the Markov model has a modular structure.[50] Also, for the purpose of analysis it might be useful to aggregate states into sets that describe related properties. An simple

example for aggregation is shown in Figure 9 where the model that describes all possible combinations of states of two predators has been reduced to an equivalent model that accounts only for the number of predators in the feeding state.

This leads us to the problem of representing a large number of individuals that each have a large set of states. For a representation of a large number of individuals we need to form the Cartesian product of the state set as explained in section 3.3.3 which leads to a rapid increase of the state set of the complete system. Here, it is important to consider for which number of individuals it is still warranted to represent them using an IBM—the larger the population size becomes, the less likely it is that the influence of inter-individual differences still plays a strong role. In this situation it is worth considering which groups of individuals still need to be modelled as individuals and which groups—in the interest of obtaining a parsimonious model—should better be represented following a population-based approach via differential equations. The ability to model the interactions of populations that are represented following an individual-based approach with populations that are modelled via differential equations has been one of the most important motivations for our approach.

Finally, after we have discussed the challenges of increasing the state space of the Markov model, let us consider the other component of a PDMP i.e. the system of differential equations that describes elements of our model that are represented via continuous variables. This includes populations which are not modelled via an individual-based approach as well as continuous variables similar to the example shown in section 3.3.2. When solving the partial differential equations for calculating the probability densities ρ_S this leads to the unusual situation that the equations depend on a large number of variables. It is difficult to predict how challenging this will be—whereas it should be possible to obtain numerical solutions even for PDEs that depend on more than a few variables, it might be more difficult to interpret the resulting probability densities. If the probability densities ρ_S will still provide valuable insight for models with a large number of continuous variables or if it is better to restrict the number of continuous variables is a question to be answered in future work.

Currently, we are working on several promising applications of PDMPs, ranging from individual-based modelling of infections, ecology and social conflict to physiology which will be presented in forthcoming publications.

In summary, we have shown how PDMPs can be used for designing IBMs which, in contrast to many other approaches to individual-based modelling can be analysed systematically using a rigorous mathematical framework. At the same time, despite relying on a fixed model architecture, PDMPs offer a high level of flexibility that enables the modeller to obtain a rich description of many characteristics of the individuals to be modelled.

Acknowledgements

The authors would like to thank two anonymous reviewers and editor Gail Wolkowicz for their very supportive comments and their encouraging feedback which greatly improved the work presented here. IS would also like to thank the organisers of the very enjoyable MPDEE 2022 conference where this work was first presented.

References

1. Volker Grimm and Steven F. Railsback. *Individual-based Modeling and Ecology*. Princeton Series in Theoretical and Computational Biology. Princeton University Press, Princeton and Oxford, 2005.
2. Steven F. Railsback and Volker Grimm. *Agent-Based and Individual-Based Modeling: A Practical Introduction*. Princeton University Press, Princeton, 2012.
3. S. Eubank, H. Guclu, V. S. A. Kumar, M. V. Marathe, A. Srinivasan, Z. Toroczkai, and N. Wang. Modelling disease outbreaks in realistic urban social networks. *Nature*, 429(6988):180–184, 2004. cited By (since 1996)590.
4. N. M. Ferguson, D. A. T. Cummings, S. Cauchemez, C. Fraser, S. Riley, A. Meeyai, S. Iamsirithaworn, and D. S. Burke. Strategies for containing an emerging influenza pandemic in southeast asia. *Nature*, 437(7056):209–214, 2005. cited By (since 1996)814.
5. Leonardo López, Maximiliano Fernández, Andrea Gómez, and Leonardo Giovanini. An influenza epidemic model with dynamic social networks of agents with individual behaviour. *Ecological Complexity*, 41:100810, 2020.
6. James M. Osborne, Alexander G. Fletcher, Joe M. Pitt-Francis, Philip K. Maini, and David J. Gavaghan. Comparing individual-based approaches to modelling the self-organization of multicellular tissues. *PLOS Computational Biology*, 13(2):1–34, 02 2017.
7. J. Groeneveld, B. Müller, C.M. Buchmann, G. Dressler, C. Guo, N. Hase, F. Hoffmann, F. John, C. Klassert, T. Lauf, V. Liebelt, H. Nolzen, N. Pannicke, J. Schulze, H. Weise, and N. Schwarz. Theoretical foundations of human decision-making in agent-based land use models – a review. *Environmental Modelling & Software*, 87:39–48, 2017.
8. Andrea K Knittel, Rick L Riolo, and Rachel C Snow. Development and evaluation of an agent-based model of sexual partnership. *Adaptive Behavior*, 19(6):425–450, 2011.
9. Ivo Siekmann and James M. Osborne. Editorial: Do individuals matter? - individual-based versus population-based models applied to biology and health. *Frontiers in Applied Mathematics and Statistics*, 9, 2023.
10. Joshua C. Kynaston, Christian A. Yates, Anna V. F. Hekkink, and Chris Guiver. The regime-conversion method: a hybrid technique for simulating well-mixed chemical reaction networks. *Frontiers in Applied Mathematics and Statistics*, 9, 2023.
11. Robert Müller, Arthur Boutillon, Diego Jahn, Jörn Starruß, Nicolas B. David, and Lutz Brusch. Collective cell migration due to guidance-by-followers is robust to multiple stimuli. *Frontiers in Applied Mathematics and Statistics*, 9, 2023.
12. C. J. M. Musters, Don L. DeAngelis, Jeffrey A. Harvey, Wolf M. Mooij, Peter M. van Bodegom, and Geert R. de Snoo. Enhancing the predictability of ecology in a changing world: A call for an organism-based approach. *Frontiers in Applied Mathematics and Statistics*, 9, 2023.
13. Yuanming Lu, Junfei Xia, Lukas J. Magee, and Donald L. DeAngelis. Seed dispersal and tree legacies influence spatial patterns of plant invasion dynamics. *Frontiers in Applied Mathematics and Statistics*, 9, 2023.

14. Aisling J. Daly, Lander De Visscher, Jan M. Baetens, and Bernard De Baets. Quo vadis, agent-based modelling tools? *Environmental Modelling & Software*, 157:105514, 2022.
15. Volker Grimm, Uta Berger, Finn Bastiansen, Sigrunn Eliassen, Vincent Ginot, Jarl Giske, John Goss-Custard, Tamara Grand, Simone K. Heinz, Geir Huse, Andreas Huth, Jane U. Jepsen, Christian Jørgensen, Wolf M. Mooij, Birgit Müller, Guy Pe'er, Cyril Piou, Steven F. Railsback, Andrew M. Robbins, Martha M. Robbins, Eva Rossmanith, Nadja Rüger, Espen Strand, Sami Souissi, Richard A. Stillman, Rune Vabø, Ute Visser, and Donald L. DeAngelis. A standard protocol for describing individual-based and agent-based models. *Ecological Modelling*, 198(1):115–126, 2006.
16. Volker Grimm, Uta Berger, Donald L. DeAngelis, J. Gary Polhill, Jarl Giske, and Steven F. Railsback. The odd protocol: A review and first update. *Ecological Modelling*, 221(23):2760–2768, 2010.
17. Volker Grimm, Steven F. Railsback, Christian E. Vincenot, Uta Berger, Cara Gallagher, Donald L. DeAngelis, Bruce Edmonds, Jiaqi Ge, Jarl Giske, Jürgen Groeneveld, Alice S.A. Johnston, Alexander Milles, Jacob Nabe-Nielsen, Gary Polhill, Viktoriia Radchuk, Marie-Sophie Rohwäder, Richard A. Stillman, Jan C. Thiele, and Daniel Ayllón. The ODD protocol for describing agent-based and other simulation models: A second update to improve clarity, replication, and structural realism. *Journal of Artificial Societies and Social Simulation*, 23(2):7, 2020.
18. Volker Grimm, Jacqueline Augusiak, Andreas Focks, Béatrice M. Frank, Faten Gabsi, Alice S.A. Johnston, Chun Liu, Benjamin T. Martin, Mattia Meli, Viktoriia Radchuk, Pernille Thorbek, and Steven F. Railsback. Towards better modelling and decision support: Documenting model development, testing, and analysis using trace. *Ecological Modelling*, 280:129–139, 2014. Population Models for Ecological Risk Assessment of Chemicals.
19. Yu. A. Kuznetsov. *Elements of applied bifurcation theory*, volume 112 of *Applied Mathematical Sciences*. Springer, Berlin, 1995.
20. S. Wiggins. *Introduction to applied nonlinear dynamical systems and chaos*, volume 2 of *Texts in Applied Mathematics*. Springer, New York, 2 edition, 2003.
21. Eusebius J. Doedel. Lecture Notes on Numerical Analysis of Nonlinear Equations. In Bernd Krauskopf, Hinke Osinga, and Jorge Galán-Vioque, editors, *Numerical Continuation Methods for Dynamical Systems: Path following and boundary value problems*, Springer Complexity, chapter 1, pages 1–49. Springer, Dordrecht, The Netherlands, 2007.
22. A. Dhooge, W. Govaerts, Yu.A. Kuznetsov, W. Mestrom, A.M. Riet, and B. Sautois. *Matcont and cl_matcont: Continuation toolboxes in matlab.*, 2006.
23. A. Dhooge, W. Govaerts, Yu.A. Kuznetsov, and B. Sautois. *Matcont: A matlab package for dynamical systems with applications to neural activity*, 2006.
24. Jaime Cisternas, C. William Gear, Simon Levin, and Ioannis G. Kevrekidis. Equation-free modelling of evolving diseases: coarse-grained computations with individual-based models. *Proceedings of the Royal Society A*, 460:2761–2779, 2004.
25. A. C. Tsoumanis, C. I. Siettos, G. V. Bafas, and I. G. Kevrekidis. Equation-free multiscale computations in social networks: from agent-based modeling to coarse-grained stability and bifurcation analysis. *International Journal of Bifurcation and Chaos*, 20(11):3673–3688, 2010.
26. Constantinos I. Siettos. Equation-free multiscale computational analysis of individual-based epidemic dynamics on networks. *Applied Mathematics and Computation*, 218(2):324 – 336, 2011.
27. Ivo Siekmann. Bifurcation analysis of individual-based models in population dynamics.

Ecological Complexity, 21(0):177 – 184, 2015.
28. Romina Martin and Spencer Angus Thomas. Analyzing regime shifts in agent-based models with equation-free analysis. In *International Congress on Environmental Modelling and Software*, 2016.
29. Spencer A. Thomas, David J.B. Lloyd, and Anne C. Skeldon. Equation-free analysis of agent-based models and systematic parameter determination. *Physica A: Statistical Mechanics and its Applications*, 464:27–53, 2016.
30. Patsy Haccou, Peter Jagers, and Vladimir A. Vatutin. *Branching Processes: Variation, Growth, and Extinction of Populations*. Cambridge Studies in Adaptive Dynamics. Cambridge University Press, 2005.
31. F. Schweitzer. *Brownian agents and active particles. Collective dynamics in the natural and social sciences*. Springer Series in Synergetics. Springer, Berlin, 2003.
32. Luis R. Izquierdo, Segismundo S. Izquierdo, José Manuel Galán, and José Ignacio Santos. Techniques to understand computer simulations: Markov chain analysis. *Journal of Artificial Societies and Social Simulation*, 12(1):6, 2009.
33. Reinhard Laubenbacher, Abdul S. Jarrah, Henning Mortveit, and S. S. Ravi. A mathematical formalism for agent-based modeling. In Robert A. Meyers, editor, *Encyclopedia of Complexity and Systems Science*, pages 160–176. Springer, New York, 1 edition, 2009.
34. Sven Banisch, Ricardo Lima, and Tanya Araújo. Agent based models and opinion dynamics as markov chains. *Social Networks*, 34(4):549–561, 2012.
35. Sven Banisch. *Markov Chain Aggregation for Agent-Based Models*. Understanding Complex Systems. Springer, Cham, 1 edition, 2016.
36. Wolf M. Mooij, Julien Martin, Wiley M. Kitchens, and Donald L. DeAngelis. Exploring the temporal effects of seasonal water availability on the snail kite of florida. In John A. Bissonette and Ilse Storch, editors, *Temporal Dimensions of Landscape Ecology—Wildlife Responses to Variable Resources*, chapter 9, pages 155–173. Springer, New York, USA, 2007.
37. M. H. A. Davis. Piecewise-deterministic markov processes: A general class of non-diffusion stochastic models. *Journal of the Royal Statistical Society. Series B (Methodological)*, 46(3):353–388, 1984.
38. Paul C. Bressloff and James N. Maclaurin. Stochastic hybrid systems in cellular neuroscience. *The Journal of Mathematical Neuroscience*, 8(1):12, 2018.
39. Paul C. Bressloff. *Stochastic Processes in Cell Biology—Volume 1: Molecular Processes*, volume 41 of *Interdisciplinary Applied Mathematics*. Springer, Cham, Switzerland, 2nd edition, 2021.
40. Paul C. Bressloff. *Stochastic Processes in Cell Biology—Volume 2: Cellular Processes*, volume 41 of *Interdisciplinary Applied Mathematics*. Springer, Cham, Switzerland, 2nd edition, 2021.
41. Vlastimil Křivan. Optimal foraging and predator–prey dynamics. *Theoretical Population Biology*, 49(3):265–290, 1996.
42. V. Křivan and A. Sikder. Optimal foraging and predator-prey dynamics, ii. *Theoretical Population Biology*, 55(2):111–126, 1999. cited By 87.
43. V. Křivan and J. Eisner. Optimal foraging and predator-prey dynamics iii. *Theoretical Population Biology*, 63(4):269–279, 2003. cited By 64.
44. J. W. Thomas. *Numerical partial differential equations: Finite difference methods*, volume 22 of *Texts in Applied Mathematics*. Springer, New York, 1995.
45. Aslak Tveito and Glenn T. Lines. *Computing Characterizations of Drugs for Ion Channels and Receptors Using Markov Models*, volume 111 of *Lecture Notes in Computational Science and Engineering*. Springer, 1 edition, 2016.

46. N.G. van Kampen. *Stochastic processes in physics and chemistry*. North-Holland, Amsterdam, 3rd edition, 1981.
47. Shin-Ho Chung and Rodney A. Kennedy. Coupled Markov chain model: Characterization of membrane channel currents with multiple conductance sublevels as partially coupled elementary pores. *Mathematical Biosciences*, 133(2):111 – 137, 1996.
48. FG Ball, RK Milne, and GF Yeo. Stochastic models for systems of interacting ion channels. *IMA JOURNAL OF MATHEMATICS APPLIED IN MEDICINE AND BIOLOGY*, 17(3):263–293, SEP 2000.
49. Laura Jula Vanegas, Benjamin Eltzner, Daniel Rudolf, Miroslav Dura, Stephan E. Lehnart, and Axel Munk. Analyzing cross-talk between superimposed signals: Vector norm dependent hidden markov models and applications. arXiv:2103.06071, 2022.
50. Ivo Siekmann, Mark Fackrell, Edmund J. Crampin, and Peter Taylor. Modelling modal gating of ion channels with hierarchical markov models. *Proceedings of the Royal Society of London A*, 472:20160122, 2016.
51. M. Abramowitz and I. A. Stegun, editors. *Handbook of Mathematical Functions: With Formulas, Graphs, and Mathematical Tables*. Dover Books, 10th edition, 1972.
52. W. N. Bailey. *Generalised Hypergeometric Series*, volume 32 of *Cambridge Tracts in Mathematics and Mathematical Physics*. Cambridge University Press, 1935.

Appendix A. Derivation of stationary densities $\rho_{\mathrm{R}}^{\infty}(x)$ and $\rho_{\mathrm{F}}^{\infty}(x)$

A.1. *Unnormalised densities*

For the stationary densities we have $\frac{\partial}{\partial t}\begin{pmatrix}\rho_{\mathrm{R}}(t,x)\\ \rho_{\mathrm{F}}(t,x)\end{pmatrix} = \mathbf{0}$ so that we need to solve the equations

$$\frac{d}{dx} f_{\mathrm{R}}(x)\rho_{\mathrm{R}}^{\infty}(x) = -k_{\mathrm{RF}}\rho_{\mathrm{R}}^{\infty}(x) + k_{\mathrm{FR}}\rho_{\mathrm{F}}^{\infty}(x), \tag{A.1}$$

$$\frac{d}{dx} f_{\mathrm{F}}(x)\rho_{\mathrm{F}}^{\infty}(x) = k_{\mathrm{RF}}\rho_{\mathrm{R}}^{\infty}(x) - k_{\mathrm{FR}}\rho_{\mathrm{F}}^{\infty}(x). \tag{A.2}$$

By summing (A.1) and (A.2) we obtain the simple equation

$$\frac{d}{dx}\left(f_{\mathrm{R}}(x)\rho_{\mathrm{R}}^{\infty}(x) + f_{\mathrm{F}}(x)\rho_{\mathrm{F}}^{\infty}(x)\right) = 0. \tag{A.3}$$

The boundary conditions state that both densities shall vanish at $x = 0$ and $x = 1$ so that $f_{\mathrm{R}}(x)\rho_{\mathrm{R}}^{\infty}(x) + f_{\mathrm{F}}(x)\rho_{\mathrm{F}}^{\infty}(x) = 0$ for $x \in [0,1]$ and it follows, after solving for $\rho_{\mathrm{F}}^{\infty}$:

$$\rho_{\mathrm{F}}^{\infty}(x) = -\frac{f_{\mathrm{R}}(x)}{f_{\mathrm{F}}(x)}\rho_{\mathrm{R}}^{\infty}(x). \tag{A.4}$$

Using (A.4) we can now eliminate $\rho_{\mathrm{F}}^{\infty}(x)$ in (A.1) so that we obtain a linear differential equation in $\rho_{\mathrm{R}}^{\infty}(x)$:

$$\frac{d}{dx} f_{\mathrm{R}}(x)\rho_{\mathrm{R}}^{\infty}(x) = -\left(k_{\mathrm{RF}} + k_{\mathrm{FR}}\frac{f_{\mathrm{R}}(x)}{f_{\mathrm{F}}(x)}\right)\rho_{\mathrm{R}}^{\infty}(x). \tag{A.5}$$

After differentiating on the left-hand side of (A.5) the differential equation simplifies to

$$\frac{d}{dx}\rho_{\mathrm{R}}^{\infty}(x) = -\underbrace{\left(\frac{k_{\mathrm{RF}}}{f_{\mathrm{R}}(x)} + \frac{k_{\mathrm{FR}}}{f_{\mathrm{F}}(x)} + \frac{\frac{d}{dx}f_{\mathrm{R}}(x)}{f_{\mathrm{R}}(x)}\right)}_{a(x)}\rho_{\mathrm{R}}^{\infty}(x), \tag{A.6}$$

which has the solution

$$\rho_{\mathrm{R}}^{\infty}(x) = C\exp\left(-\int a(x)dx\right). \tag{A.7}$$

Thus, we now have to integrate $a(x)$. Taking into account $f_{\mathrm{R}}(x) = x(1-x)$ and $f_{\mathrm{F}}(x) = x(1-x) - dx$ we rewrite $a(x)$ so that the integral can be easily calculated:

$$a(x) = \frac{k_{\mathrm{RF}} - \frac{k_{\mathrm{FR}}}{d-1} + 1}{x} + \frac{k_{\mathrm{RF}} - 1}{1-x} + \frac{\frac{k_{\mathrm{FR}}}{d-1}}{x+d-1},\ d \neq 1. \tag{A.8}$$

Note that (A.8) can be used for both $d > 1$ and $d < 1$. Only the case $d = 1$ needs to be treated separately. The anti-derivatives of all terms in (A.8) are all log functions and we obtain:

$$\begin{aligned}\int a(x)dx = &\left(k_{\mathrm{RF}} - \frac{k_{\mathrm{FR}}}{d-1} + 1\right)\log(x)\\ &+ (1-k_{\mathrm{RF}})\log(1-x) + \left(\frac{k_{\mathrm{FR}}}{d-1}\right)\log(x+d-1),\ d \neq 1.\end{aligned} \tag{A.9}$$

Substituting (A.9) in the solution (A.7) yields

$$\rho_{\mathrm{R}}^{\infty}(x) = Cx^{-\left(k_{\mathrm{RF}} - \frac{k_{\mathrm{FR}}}{d-1} + 1\right)}(1-x)^{k_{\mathrm{RF}}-1}(x+d-1)^{-\frac{k_{\mathrm{FR}}}{d-1}}. \tag{A.10}$$

Finally, we obtain $\rho_{\mathrm{F}}^{\infty}(x)$ using (A.4):

$$\rho_{\mathrm{F}}^{\infty}(x) = C\left(-\frac{f_{\mathrm{R}}(x)}{f_{\mathrm{F}}(x)}\right)x^{-\left(k_{\mathrm{RF}} - \frac{k_{\mathrm{FR}}}{d-1} + 1\right)}(1-x)^{k_{\mathrm{RF}}-1}(x+d-1)^{-\frac{k_{\mathrm{FR}}}{d-1}} \tag{A.11}$$

$$= C\left(\frac{1-x}{x+d-1}\right)x^{-\left(k_{\mathrm{RF}} - \frac{k_{\mathrm{FR}}}{d-1} + 1\right)}(1-x)^{k_{\mathrm{RF}}-1}(x+d-1)^{-\frac{k_{\mathrm{FR}}}{d-1}} \tag{A.12}$$

$$= Cx^{-\left(k_{\mathrm{RF}} - \frac{k_{\mathrm{FR}}}{d-1} + 1\right)}(1-x)^{k_{\mathrm{RF}}}(x+d-1)^{-\frac{k_{\mathrm{FR}}}{d-1}-1}. \tag{A.13}$$

A.2. *Calculation of the normalisation constant*

The solutions that we found for $\rho_{\mathrm{R}}^{\infty}(x)$ and $\rho_{\mathrm{F}}^{\infty}(x)$ are, so far, not normalised. In order, to ensure that $\rho_{\mathrm{R}}^{\infty}(x)$ and $\rho_{\mathrm{F}}^{\infty}(x)$ define a probability distribution over the space $\mathcal{S} \times [0,1]$ we need to ensure that

$$\int_0^1 (\rho_{\mathrm{R}}^{\infty}(x) + \rho_{\mathrm{F}}^{\infty}(x)dx = 1. \tag{A.14}$$

Thus, the normalisation constant can be found by choosing C such that

$$C\int_0^1 \left(x^{-\left(k_{\mathrm{RF}}-\frac{k_{\mathrm{FR}}}{d-1}+1\right)}(1-x)^{k_{\mathrm{RF}}-1}(x+d-1)^{-\frac{k_{\mathrm{FR}}}{d-1}}\right)dx \tag{A.15}$$

$$+\,C\int_0^1 \left(x^{-\left(k_{\mathrm{RF}}-\frac{k_{\mathrm{FR}}}{d-1}+1\right)}(1-x)^{k_{\mathrm{RF}}}(x+d-1)^{-\frac{k_{\mathrm{FR}}}{d-1}-1}\right)dx = 1. \tag{A.16}$$

We take advantage of the Euler type integral formula, see, for example, Abramowitz and Stegun, section 15.3.1[51] or Bailey:[52]

$$\mathrm{B}(b,c-b)\;{}_2F_1(a,b;c,z) = \int_0^1 x^{b-1}(1-x)^{c-b-1}(1-zx)^{-a}dx, \tag{A.17}$$

for which we must have $\Re(c) > \Re(b) > 0$. Here, B is the beta function and ${}_2F_1$ the hypergeometric function. It follows

- for $\rho_{\mathrm{R}}^{\infty}(x)$ (2.6) that $a = \frac{k_{\mathrm{FR}}}{d-1}$, $b = \frac{k_{\mathrm{FR}}}{d-1} - k_{\mathrm{RF}}$ and $c = \frac{k_{\mathrm{FR}}}{d-1}$
- for $\rho_{\mathrm{F}}^{\infty}(x)$ (2.7) that $a = \frac{k_{\mathrm{FR}}}{d-1}+1$, $b = \frac{k_{\mathrm{FR}}}{d-1} - k_{\mathrm{RF}}$ and $c = \frac{k_{\mathrm{FR}}}{d-1}+1$

In order to find z we have to factor out $(d-1)^{-a}$ and we obtain $z = \frac{1}{1-d}$ for both $\rho_{\mathrm{R}}^{\infty}(x)$ and $\rho_{\mathrm{F}}^{\infty}(x)$. With these choices for a, b, c and z we find:

$$C(d-1)^{-\frac{k_{\mathrm{FR}}}{d-1}}\,\mathrm{B}\left(\tfrac{k_{\mathrm{FR}}}{d-1}-k_{\mathrm{RF}},k_{\mathrm{RF}}\right){}_2F_1\left(\tfrac{k_{\mathrm{FR}}}{d-1},\tfrac{k_{\mathrm{FR}}}{d-1}-k_{\mathrm{RF}};\tfrac{k_{\mathrm{FR}}}{d-1},\tfrac{1}{1-d}\right)$$

$$+\,C(d-1)^{-\frac{k_{\mathrm{FR}}}{d-1}-1}\,\mathrm{B}\left(\tfrac{k_{\mathrm{FR}}}{d-1}-k_{\mathrm{RF}},k_{\mathrm{RF}}+1\right){}_2F_1\left(\tfrac{k_{\mathrm{FR}}}{d-1}+1,\tfrac{k_{\mathrm{FR}}}{d-1}-k_{\mathrm{RF}};\tfrac{k_{\mathrm{FR}}}{d-1}+1,\tfrac{1}{1-d}\right) = 1 \tag{A.18}$$

and C can be obtained by solving (A.18).

Appendix B. Expectations x_{R} and x_{F}

Integrating $\frac{1}{p_{\mathrm{R}}^{\infty}}\int_0^1 x\cdot\rho_{\mathrm{R}}^{\infty}(x)dx$ yields $p_{\mathrm{R}}^{\infty}\cdot\mathbb{E}[x_{\mathrm{R}}]$ where p_{R}^{∞} is the stationary probability of the state R. Thus, we calculate

$$\begin{aligned}\mathbb{E}[x_{\mathrm{R}}] &= \frac{1}{p_{\mathrm{R}}^{\infty}}\int_0^1 x\cdot\rho_{\mathrm{R}}^{\infty}(x)dx \\ &= \frac{C}{p_{\mathrm{R}}^{\infty}}\int_0^1 x\cdot x^{-\left(k_{\mathrm{RF}}-\frac{k_{\mathrm{FR}}}{d-1}+1\right)}(1-x)^{k_{\mathrm{RF}}-1}(x+d-1)^{-\frac{k_{\mathrm{FR}}}{d-1}}dx\end{aligned} \tag{B.1}$$

and find, with the Euler type integral (A.17), that (B.1) evaluates to $\mathrm{B}(b,c-b)\;{}_2F_1(a,b;c,z)$ where

- $a = \frac{k_{\mathrm{FR}}}{d-1}$, $b = \frac{k_{\mathrm{FR}}}{d-1} - k_{\mathrm{RF}}+1$, $c = \frac{k_{\mathrm{FR}}}{d-1}+1$ and $z = \frac{1}{1-d}$ for $\mathbb{E}[x_{\mathrm{R}}]$ and, analogously,
- $a = \frac{k_{\mathrm{FR}}}{d-1}+1$, $b = \frac{k_{\mathrm{FR}}}{d-1} - k_{\mathrm{RF}}+1$, $c = \frac{k_{\mathrm{FR}}}{d-1}+2$ and $z = \frac{1}{1-d}$ for $\mathbb{E}[x_{\mathrm{F}}]$.

With these choices for the parameters a, b, c and z we obtain the expressions for $\mathbb{E}[x_{\mathrm{R}}]$ and $\mathbb{E}[x_{\mathrm{F}}]$ given in (2.10), (2.11).